

# RSC Advances

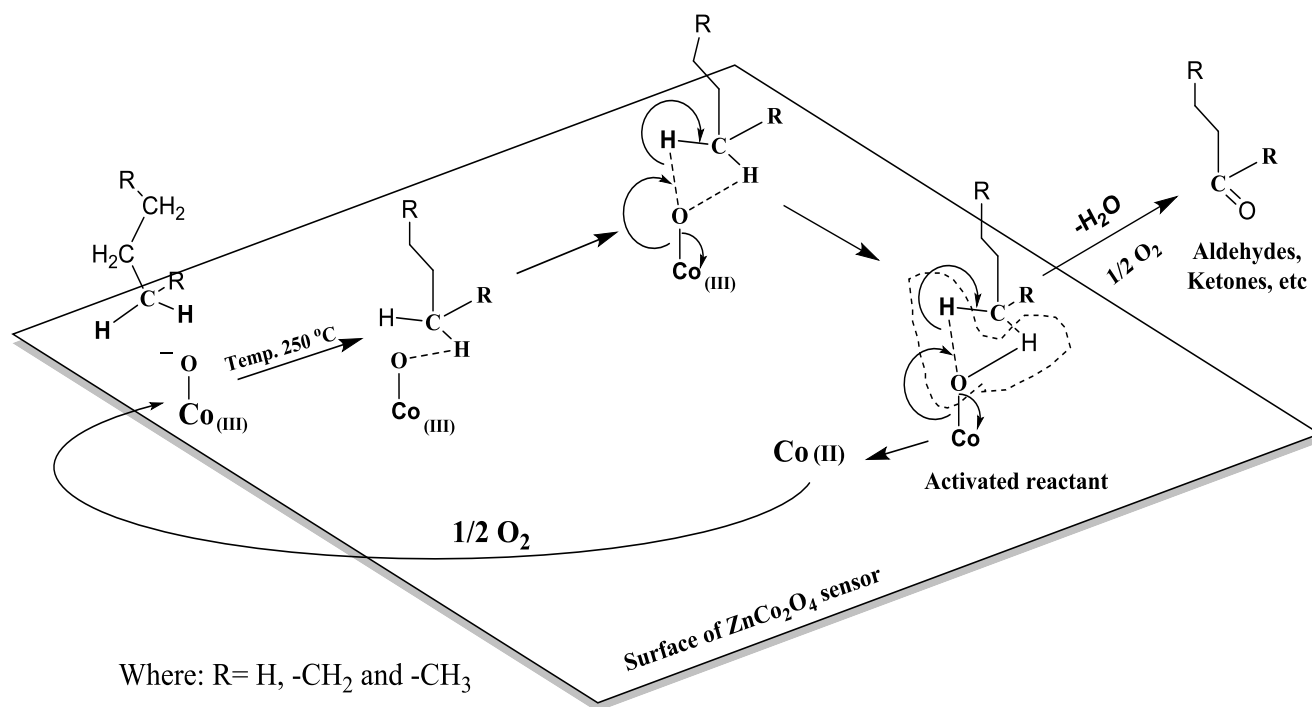


This is an *Accepted Manuscript*, which has been through the Royal Society of Chemistry peer review process and has been accepted for publication.

*Accepted Manuscripts* are published online shortly after acceptance, before technical editing, formatting and proof reading. Using this free service, authors can make their results available to the community, in citable form, before we publish the edited article. This *Accepted Manuscript* will be replaced by the edited, formatted and paginated article as soon as this is available.

You can find more information about *Accepted Manuscripts* in the [Information for Authors](#).

Please note that technical editing may introduce minor changes to the text and/or graphics, which may alter content. The journal's standard [Terms & Conditions](#) and the [Ethical guidelines](#) still apply. In no event shall the Royal Society of Chemistry be held responsible for any errors or omissions in this *Accepted Manuscript* or any consequences arising from the use of any information it contains.



Cite this: DOI: 10.1039/c0xx00000x

www.rsc.org/xxxxxx

PAPER

## Effect of composition zinc:cobalt in $\text{ZnCo}_2\text{O}_4$ spinel on highly selective liquefied petroleum gas sensor at low and high temperature conditions

Kalpana B. Gawande<sup>a</sup>, Sandeep B. Gawande<sup>a</sup>, Sanjay R. Thakare<sup>a</sup>, Vivek R. Mate<sup>b,c,d\*</sup>, Sunil R. Kadam<sup>b</sup>, Bharat B. Kale<sup>b</sup> and Milind V. Kulkarni<sup>b</sup>

Received (in XXX, XXX) Xth XXXXXXXXX 20XX, Accepted Xth XXXXXXXXX 20XX

DOI: 10.1039/b000000x

The nano  $\text{ZnCo}_2\text{O}_4$  mixed phase materials were synthesized at varying zinc and cobalt ratios such as 1:1, 1:1.5, 1:2, 1:2.5 and 1:3. With change in composition from 1:1 to 1:2.5 gas sensing response characteristics increased two times (from 40 to 77.5), while at higher zinc cobalt composition (1:3) it shown saturation point (about 80). This specifies optimal cobalt loading (1:2.5) is leads to two times enhancement in redox ability (from 174 to 346 mmole) and number of active sites this upshot significantly helps to sensing response much lower 10 ppm and saturation point at higher 60 ppm LPG concentration. Further, nano  $\text{ZnCo}_2\text{O}_4$  (with zinc and cobalt ratios 1:2.5) material exhibited excellent response (~80–90 s), rapid recovery time (~65–75 s), excellent repeatability (fourth cycle), good selectivity (for LPG), higher gas response (~77.5), short and lower as well as higher operating temperature (from 30 to 250 °C). The results clearly reveal that by tuning cobalt composition in  $\text{Zn}_x\text{Co}_{2-x}\text{O}_4$ , we can achieve maximum sensing efficiency and repeatability.

### Introduction

Liquefied petroleum gas (LPG) is an important chemical raw material widely used as fuel for domestic and industrially to provide a clean source of energy. It is a combustible gas which mainly consists of butane, propane, propylene, butylene, ethylene methane and carbon monoxide.<sup>1</sup> However, LPG is dangerous because of its extremely flammable risks.<sup>1–4</sup> LPG leakage may take place at any facilities for LPG production, transportation, storage and application. Therefore, LPG leakage monitoring is extremely important in these facilities.

In previous decade, various efforts have been made to improve the chemical sensing activities of the sensing materials, only a few effective sensing materials for LPG gas have been reported.<sup>1–4</sup>

This has stimulated considerable interest for scientific research to develop simple and cost-effective chemical sensors for the detection of LPG in recent years and many efforts, in this field, are today devoted to the synthesis of novel sensing materials with enhanced performance.<sup>2,5–8</sup> Up till now, the semiconductors

especially metal oxide have been widely investigated as gas sensing materials because of their low cost and power consumption, simplicity of fabrication and use, versatility in detecting a wide range of flammable/toxic gases, and stability in harsh environments.<sup>9,10</sup> Recent studies reveal that the nano materials have ultrahigh sensitivity to different gases due to their small particle size and large surface was performed using different morphology (i.e. in the form of nanorods, nanoparticles, nanowires, warm like, etc.) of single and mix phase metal oxides materials like Pd, Fe, Cd, Sn, Cu, In, Pt, Zn, Cd, In and Co.<sup>1–4,6–28</sup> However, major drawbacks associated with these systems are: use of expensive noble metal, multistep synthesis, sensor activity limited to room temperature, sensor deactivation due to formation of metal inactive species and blockage of active species by chemi-adsorbed unreacted intermediates with active species.<sup>29,30</sup>

Recently, our group has been focusing on developing efficient semiconductor and efficient catalytic material for the solar light harvesting.<sup>31,32</sup> The  $\text{Co}_3\text{O}_4$  and  $\text{ZnO}$  nano particles serve as the active sites of redox reactions, which result in high activity for the gas sensing materials.<sup>33</sup> Cobalt and zinc are the most attractive elements for the gas sensing materials because of its strong ability to activate molecular gases (oxygen, LPG,  $\text{CO}_2$ , etc) and is also more cost effective than the noble metals. In spite of these facts, a single report is found on LPG gas sensing using mix phase  $\text{ZnCo}_2\text{O}_4$  as a sensing material.<sup>1</sup> This study shown results of  $\text{ZnCo}_2\text{O}_4$  sensing materials only at high temperature. Whereas, other aspects such as optimization of cobalt and zinc composition in  $\text{ZnCo}_2\text{O}_4$  in order to enhance surface active species, stability/reusability, interaction of LPG molecule over

<sup>a</sup>Department of Chemistry, Govt. Institute of Science, Civil Lines, Nagpur, 440001, India;

<sup>b</sup>Centre for Materials for Electronic Technology, Panchawati, off Pashan Road, Pune, 411008, India, Fax: +91-20-2589 8085; Tel: +91-20-25898390;

<sup>c</sup>Department of Chemistry, Visvesvaraya National Institute of Technology, India +91- 0712-2801316 Fax : + 91-712-2223230.

<sup>d</sup>Department of Chemistry, National Institute of Technology Silchar, India +91-3842- 224879; Fax: + 91-3842- 224797.

<sup>e</sup>E-mail: vivekmate07@gmail.com

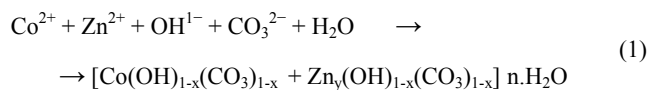
†Electronic Supplementary Information (ESI) available:

semiconductor via mechanistic way, sensing response at low as well high concentration and temperature not explicate well.

In order to overcome these problems associated with existing sensor materials, we have developed ZnCo<sub>2</sub>O<sub>4</sub> nano materials with varying cobalt and zinc composition. Furthermore in order to achieve more surface active sites, uniform crystallite size and high surface area sample is heat treated at different calcination temperature.<sup>30</sup> Hence, we prepared mix phase zinc cobalt oxide these samples were then evaluated for gas sensing at room temperature as well for high temperature for gases such as LPG, H<sub>2</sub>, ethanol, CO, CO<sub>2</sub>, and NH<sub>3</sub>. The nano-structured ZnCo<sub>2</sub>O<sub>4</sub> catalyst prepared under optimized conditions exhibited excellent gas sensing characteristics. Prepared catalysts were characterized by various techniques like TGA, XRD, XPS, HRTEM and temperature programmed reduction (TPR) measurement.

## Experimental

The synthesis of nano ZnCo<sub>2</sub>O<sub>4</sub> done using already reported method.<sup>30,34,35</sup> For the synthesis of Co<sub>3</sub>O<sub>4</sub> nanorods, the cobalt hydroxyl carbonate precursor was prepared through a low cost chemical co-precipitation/digestion method in alkaline conditions maintaining a pH ~7–8 at 60 °C. The solubility diagram for cobalt–water–carbonate system was reported by Lewis *et al.*,<sup>36</sup> which reveals the precipitation of water free cobalt carbonate above 160 °C. However, cobalt hydroxyl carbonate is preferentially precipitated at room temperature in the pH range of 7.5–10.0. It has been reported that the cobalt hydroxyl carbonate precursor particles are not well crystallized at room temperature.<sup>37</sup> Therefore, we have certain to carry out co-precipitation/digestion reaction at 60 °C to obtain better crystallinity in cobalt hydroxyl carbonate precursor. Following the same procedure, we have made an attempt to prepare the mixed precursor in alkaline conditions maintaining a pH ~7–8 at 60 °C. When potassium carbonate, cobaltus nitrate and zinc nitrate solutions are separately dropped to stirred distilled water kept at 60 °C, the following chemical reaction occurs to precipitate a mixed precursor consisting of cobalt hydroxyl carbonate and zinc hydroxyl carbonate at pH ~7-8.



As stoichiometric quantities such as 1:1, 1:1.5, 1:2, 1:2.5 and 1:3 in ratio of zinc and cobalt cationic solutions were used during preparation, it is anticipated that mixed precursor (cobalt hydroxyl carbonate + zinc hydroxyl carbonate) was precipitated by reaction (1) in stoichiometric quantity with uniform mixing of respective components. It is reported that the zinc hydroxyl carbonate with composition {Zn<sub>4</sub>(OH)<sub>6</sub>(CO<sub>3</sub>)•H<sub>2</sub>O} is precipitated at pH ~7.5–8.0 provided a careful control of factors such as M<sup>2+</sup> and/or M<sup>2+</sup>/M<sup>3+</sup> ions concentration, their ratio, pH and temperature are maintained to obtain single phase product during synthesis. As stoichiometric quantities of M<sup>2+</sup> and/or M<sup>2+</sup>/M<sup>3+</sup> ions were used for the synthesis of ZnCo<sub>2</sub>O<sub>4</sub> spinel in the present study, therefore, it is reasonable to expect that the mixed precursor with composition shown by reaction (1) will be precipitated during our synthesis protocol. This importance of this process is nano spinel (mixed oxide) material prepared

without any templates or capping and calcining the single molecular precursors at low temperature in air.

The structure of the calcined sample ZC-1-5 was investigated by using X-ray diffraction (XRD) technique. The X-ray diffraction patterns were recorded with a Rigaku diffractometer (Miniflex Model, Rigaku, Japan) (Cu K<sub>alpha</sub> λ= 0.1542 nm). The high resolution transmission electron microscopy (HRTEM) was used to determine the particle size and the morphology of the nano-sized powder with JEOL 1200 EX. The X-ray photoelectron spectroscopy (XPS) analysis was carried out using a V.G. Microtech Scientific spectrometer, ESCA 3000, U.K. equipped with two ultrahigh vacuum chambers. The pressure in the chambers during the experiments was about 10<sup>-9</sup> Pa. The XPS spectra were recorded with monochromatized Mg K radiation (photon energy = 1253.6 eV) at a constant 50 eV pass energy. The core level binding energies were corrected with the C 1s binding energy of 284.6 eV. The nanostructured ZnCo<sub>2</sub>O<sub>4</sub> powder was pressed into pellets under a pressure of 15 MPa and the ohmic contacts were made with the help of silver paste to form the sensing element. The gas sensing studies were carried out on these sensing elements in a static gas chamber to sense LPG in air ambient. The sensing element was kept directly on a heater in the gas chamber and the temperature was varied from 50 to 400 °C. The temperature of the sensing element was monitored by chromel-alumel thermocouple placed in contact with the sensor. The known volume of the LPG was introduced into the gas chamber prefilled with air and it was maintained at atmospheric pressure. The electrical resistance of the sensing element was measured before and after exposure to LPG using a sensitive digital multimeter (METRAVI 603). The performance of the sensing element is presented in terms of gas response (S), which is defined as:

$$S = \frac{R_{gas}}{R_{air}} \quad (2)$$

Where,  $R_{air}$  and  $R_{gas}$  are the electrical resistance values of the sensor element in air and in the presence of LPG gas, respectively.

## Results and discussion

### XRD results

XRD patterns of ZnCo<sub>2</sub>O<sub>4</sub> spinel samples with various compositions (Zn:Co from 1:1 to 1:3) calcined at 500 °C are presented in Fig. 1. All the samples reveal the diffraction peaks at 2θ = 31.2° (220), 36.1° (311), 44.7° (400), 59.1° (422) and 65.1° (511), which were attributed to the spinel phase of ZnCo<sub>2</sub>O<sub>4</sub> (\*) and ZnO (#) phases. The calculated lattice parameter for all the samples was found to be 8.101 Å that matched with the reported value for the spinel ZnCo<sub>2</sub>O<sub>4</sub> and ZnO phases (JCPDS 81-2299 and 80-0075) respectively. With change in Zn:Co ratio from 1:1 to 1:3, slight decrease in peak broadening and increase in peak intensity was observed for the peaks at 2θ = 31.2° (220), 36.1° (311), 44.7° (400), 59.16° (422) and 65.12° (511), indicating improvement in the crystallinity. Crystallite sizes of ZC-1 to ZC-5 samples were calculated for most intense peak at 2θ = 36.1° (311) using the Scherrer equation and were found to be ~20, 31, 38, 46 and 61 nm respectively. Thus, increase in crystallite size for the samples, ZC-2, ZC-3, ZC-4 and ZC-5 was mainly due to

the restructuring of the surface at 500 °C.<sup>32,38</sup>

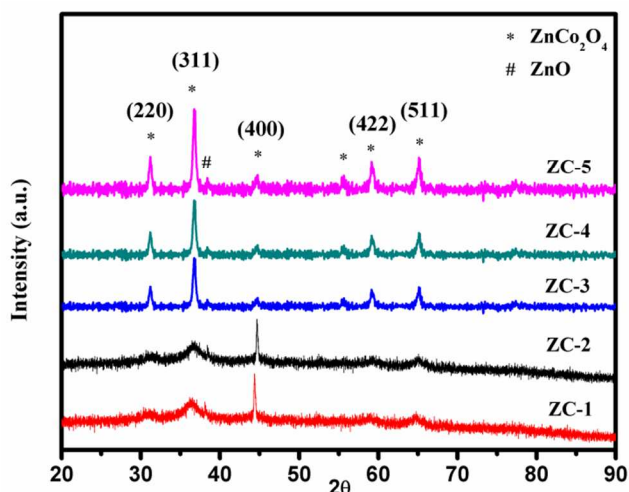


Fig. 1. XRD pattern of nanostructured ZnCo<sub>2</sub>O<sub>4</sub> prepared with different Zn:Co compositions.

### Thermal gravimetric analysis

Fig. 2 depicts the TGA curve of the as-prepared mixed precursor, which exhibits two major weight losses in the temperature range 50–210 °C and 210–420 °C. In the first step, the weight loss initiates practically from room temperature to 210 °C, with a weight loss of 13% mainly due to the loss/removal of water. The second weight loss step observed from 210 °C and is continued up to 420 °C, with a weight loss of 22%. It is associated with the decarbonation proceeding during decomposition. The formation temperature is found to be comparatively lower than that reported for corresponding solid state reaction route and co-precipitation at higher pH.<sup>1,39</sup>

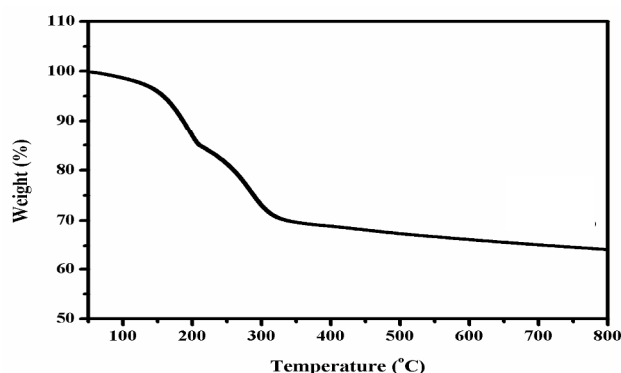


Fig. 2. TGA curve of mixed precursor.

### Surface morphology

The HRTEM images of the calcined sample ZC-4 is shown in Fig. 3. As can be seen from Fig. 3(A), mostly the ZnCo<sub>2</sub>O<sub>4</sub> particles are in the form of rods (diameter = 6–8 nm, length = 30–50 nm) with presence of few spherical crystallite particles of size ~4–7 nm in the calcined sample ZC-4, which was in good agreement with the XRD results. The parallel lattice fringes across almost all the primary particles are clearly visible (Fig. 3(A1)) which confirms the oriented aggregation of the

nanoparticles of ZnCo<sub>2</sub>O<sub>4</sub>. It is clearly seen that the aggregated ZnCo<sub>2</sub>O<sub>4</sub> rod like particles are composed of many small ZnCo<sub>2</sub>O<sub>4</sub> nanoparticles. However, the characteristic planes, (311) and (400) obtained from the SAED image (Fig.3, A2) were matched with the XRD data. Thus HRTEM and XRD result data indicates formation of the ZnCo<sub>2</sub>O<sub>4</sub> nanoparticles.

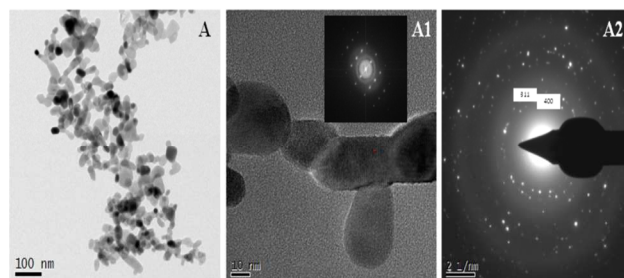


Fig. 3. HRTEM image of (A) nanorod aggregates, (A1) High resolution image of primary nano particles and (A2) SAED image of ZC-4 sample.

### Surface analysis

The XPS of ZC-4 sample is shown in Fig. 4. The Co 2p spectra showed two peaks with binding energies at 780.0 and 795.3 eV, corresponding to Co 2p<sub>3/2</sub> and Co 2p<sub>1/2</sub> core level peaks.<sup>30</sup> The Co 2p<sub>3/2</sub> and Co 2p<sub>1/2</sub> peaks separation value obtained was 15.3 eV, comparable to that observed for the Co<sub>3</sub>O<sub>4</sub> spinel (Fig. 4a). A small hump observed at a binding energy of 787.7 eV was a characteristic satellite peak of Co<sup>3+</sup>.<sup>1,40</sup> Zn 2p spectra for all the samples showed two peaks with a binding energies at 1020 and 1043 eV, which were assigned to Zn 2p<sub>3/2</sub> and Zn 2p<sub>1/2</sub> levels with splitting value of 23 eV, confirming the presence of Zn<sup>2+</sup> (Fig. 4b).<sup>31,41</sup> Hence, the above XPS and XRD result confirms the formation of ZnCo<sub>2</sub>O<sub>4</sub> spinel oxide.

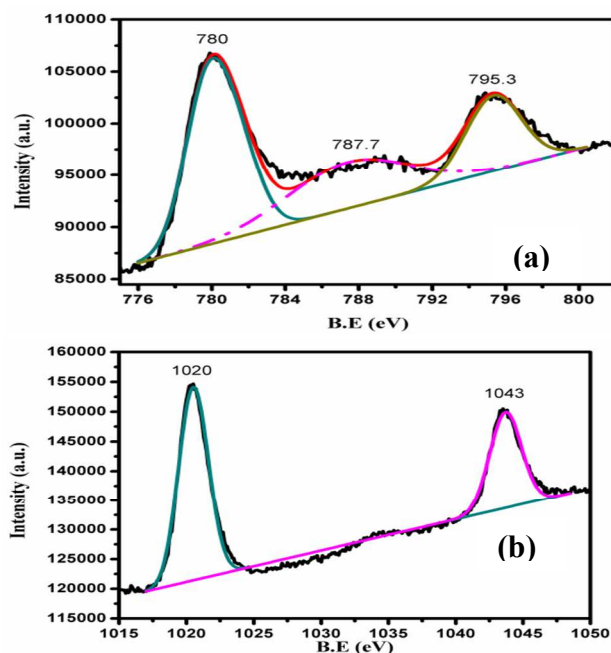


Fig. 4. XPS spectra (a) Co 2p and (b) Zn 2p of nano spinel ZnCo<sub>2</sub>O<sub>4</sub>.

### Temperature programmed reduction

The number of active sites available for gases sensing is

determined by reducibility of samples. The reducibility of the ZC-1, ZC-2, ZC-3, ZC-4 and ZC-5 catalysts was studied by H<sub>2</sub>-TPR technique (Fig. 5). The peak observed in the range of 180–300 °C in all the samples was attributed to the reduction of trivalent cobalt oxide (ZnCo<sub>2</sub>O<sub>4</sub>) to divalent cobalt oxide (CoO). Another broad peak in higher temperature range of 320–580 °C in all the samples observed could be attributed to the reduction of both divalent cobalt oxide (CoO) and zinc oxide (ZnO) to metallic cobalt (Co<sup>0</sup>) and zinc (Zn<sup>0</sup>).<sup>30,31,42</sup> While, with change in composition from ZC-1:1 to ZC-1:3 a slight increase in an intensity peak observed, due to increase in composition of cobalt in spinel Co<sub>3</sub>O<sub>4</sub>.<sup>43</sup> With change in zinc and cobalt composition from 1:1 to 1:2.5 showed increase in H<sub>2</sub> up take from 174 to 346 mmole, as further change in composition to 1:3 does not remarkably increase H<sub>2</sub> up take 357 mmole. The activities of these catalysts were found to be ~1.3, 1.7 and 2 times higher than that for nano ZC-1 spinel catalyst (Table 1). The highest reducibility of ZC-4 catalyst might be due to uniform distribution of zinc and cobalt species as observed in XPS analysis. This indicates that increase in cobalt composition improve the reducibility of the ZnCo<sub>2</sub>O<sub>4</sub> spinel and it also confirmed that redox nature was more dependent on population of Co<sup>3+</sup>/Co<sup>2+</sup> and less on Zn<sup>2+</sup> species in ZnCo<sub>2</sub>O<sub>4</sub> spinel.<sup>30</sup>

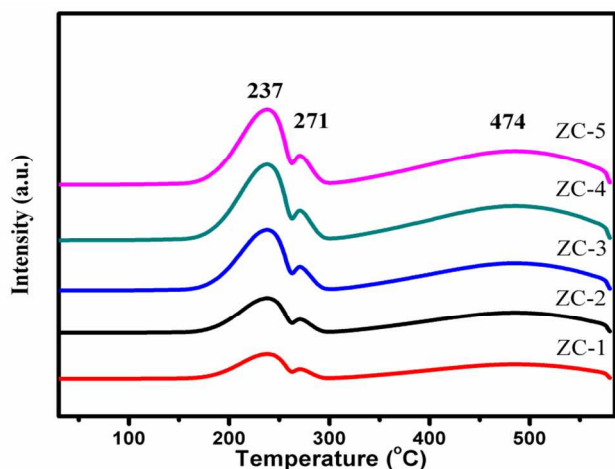


Fig. 5. TPR spectra of spinel ZnCo<sub>2</sub>O<sub>4</sub> with different compositions.

Table 1. TPR-H<sub>2</sub> uptake profiles of ZnCo<sub>2</sub>O<sub>4</sub> nano catalysts.

Catalysts	Composition (Zn:Co)	H <sub>2</sub> (mmole)
ZC-1	1:1.0	174
ZC-2	1:1.5	233
ZC-3	1:2.0	293
ZC-4	1:2.5	346
ZC-5	1:3.0	357

#### Formation mechanism of ZnCo<sub>2</sub>O<sub>4</sub> nanorods

When zinc nitrate, cobalt nitrate and potassium carbonate solutions are dropped from separate burette to distilled water at 60 °C, the following chemical reaction probably may occur to precipitate zinc cobalt hydroxyl carbonate precursor at pH ~7.0–

8.0. The XRD study confirmed the formation of polycrystalline cobalt hydroxyl carbonate with composition shown by equation:



The probable mechanism of formation of rod shaped morphology in the zinc cobalt hydroxyl carbonate precursor and resulting spinel oxide of ZnCo<sub>2</sub>O<sub>4</sub> is described as given below: initially, the zinc cobalt hydroxy carbonate particles are formed which grow with the increase in digestion time when are in contact with solution having pH ~7.0–8.0. Finally, in calcinations treatment the decarbonation takes place. Initially the small particles are formed (ZnCo<sub>2</sub>O<sub>4</sub>) and self-aligned to form rod by oriental attachment mechanism.

#### Catalyst screening

Comparisons of activities of prepared nano ZnCo<sub>2</sub>O<sub>4</sub> materials for LPG gas sensing are presented in Fig. 6. At low temperatures, the gas response is relatively low (~9.9 at 30 °C), but it increases slowly with an increase in the operating temperature in case of all samples. While, with change in sample from ZC-1 and ZC-4 showed gradual increase in gas sensing response from ~40 to 77.5 (at 250 °C), after this marginal (~80) change is observed for ZC-5 sample. This increase in gas sensing is might be due to increased surface area (from 75 to 90 m<sup>2</sup>/gm) and redox ability (174 to 346 mmole) leads to enhancement in surface active sites (ESI, Table S1). The gas response attains a maximum at ~250 °C (~77.5) and there after it start to decline with a further increase of the operating temperature (250–400 °C). This increase in gas sensing with increase in temperature (from 30 to 250 °C) is might be due to increase in collision frequency and internal pressure collectively help to increase adsorption time of LPG molecules over ZC-4, hence resulted increase in response. However, at above 250 °C instead of giving steady response it shown decrease in behaviour probably due to two possibilities such as oxidation and stability of LPG, this phenomenon explained in brief at the end of this article. Hence, an optimum operating temperature for the ZnCo<sub>2</sub>O<sub>4</sub> spinel to detect LPG is from 30 to 250 °C, which is the modest from the viewpoint of semiconducting oxide gas sensors. This indicates the nature of activities sites (both cobalt and zinc) in terms of reducibility play a dominant role in gas sensing. The activity about two times lower of ZC-1 (reducibility 174 mmole) than ZC-4 (reducibility 346 mmole) sample could be attributed to its two times lower active site observed in the TPR analysis. ZC-5 sample showed marginally higher activity than that for ZC-4 sample although its cobalt composition higher than 0.5 times more than that of ZC-4, indicating that beyond a certain value, increase in cobalt composition does not improve the gas sensing activity of the sensing material. This clearly indicates that the presence of both types of Co<sup>3+</sup> and Zn<sup>2+</sup> as well as the total reducibility is crucial in determining the gas sensing for LPG. Since, nano ZC-4 material at operating temperature of 250 °C was found to be the best catalyst because of its mixed oxidation states and highest active sites available for LPG sensing, nano ZC-4 material is consider for further study to investigate further LPG sensing properties such as response and recovery times, reproducibility and selectivity.

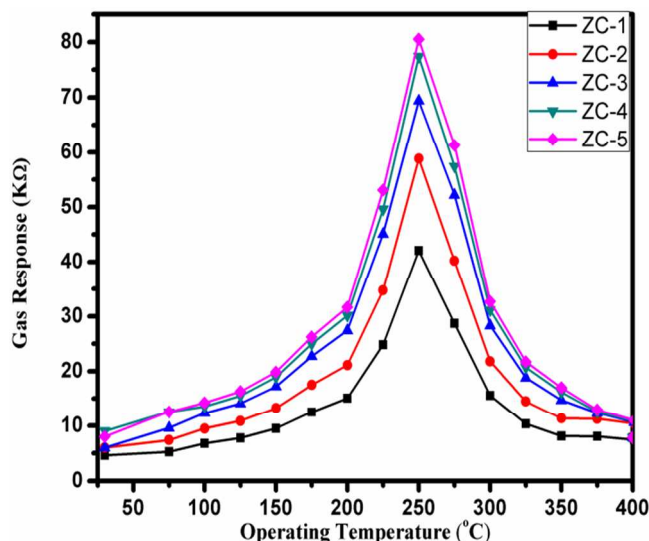


Fig. 6. Effect of temperature (from room to high temperature) on the gas response of nano  $\text{ZnCo}_2\text{O}_4$  material to 40 ppm LPG gas.

### Effect of calcination temperature

The effect of calcination temperature on the sensing performance of  $\text{ZnCo}_2\text{O}_4$  (ZC-4) sample was studied by varying the calcination temperature in a range from 300 to 600 °C, the results of which are shown in ESI, Table S2. The significant increase in LPG sensing response from 42 to 77  $\text{K}\Omega$  was observed with temperature from 300 to 500 °C, while further increase in calcinations temperature (600 °C) not increase sensing performance appreciably (79  $\text{K}\Omega$ ). However, such a dramatic increase in sensing activity might be due to the following reasons: due to calcination at higher temperature (500 °C) material surface

might be free from impurity and probable increase in active sites which is in accordance with TPR, XPS and TGA results. Thus, the above observations established that optimum calcination temperature was 500 °C for our catalyst in order to achieve the highest gas sensing activity for the LPG.

The response and recovery characteristics of the ZC-4 nano material to 40 ppm LPG is shown in Fig. 7. The response and recovery times are important parameters for evaluating the performance of gas sensors. In general, time required for the sensor resistance to change by nineteen percentage of the final resistance. It is observed that the resistance of the sensing element

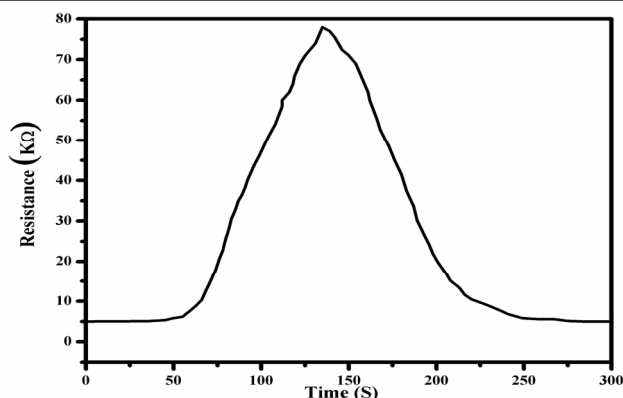


Fig. 7. Response of ZC-4 nano material to 40 ppm LPG at optimum operating temperature of 250 °C.

increases when exposed to the LPG, which suggests that ZC-4 nano material behaves as a p-type semiconductor. As can be seen from Fig. 7, the sensor responds rapidly after introduction of LPG and recovers immediately when it is exposed to air. The ZC-4 sensing material requires response time of ~80–90 s and the recovery time of ~65–75 s.

The repeatability and constancy of the ZC-4 nano material were investigated by repeating the test four times is shown in Fig. 8 and ESI Fig. S1. The ZC-4 nano material shows good reproducibility and reversibility upon repeated exposure and removal of LPG under same conditions. Additionally, the repeated tests revealed that the gas response values are maintained and the recovery abilities are not diminish after four sensing cycles. The ZC-4 nano material showed a LPG response of ~9.9 and 77.5 at 30 and 250 °C with the response and recovery times almost same (~80–90 and ~65–75 s), respectively for the exposure of 90–100 s. Hence, the ZC-4 nano material exhibits a stable and repeatable characteristic. This indicates that it can be used as a reusable sensing material for the detection of LPG not only at lower temperature but also effectively at higher temperature.

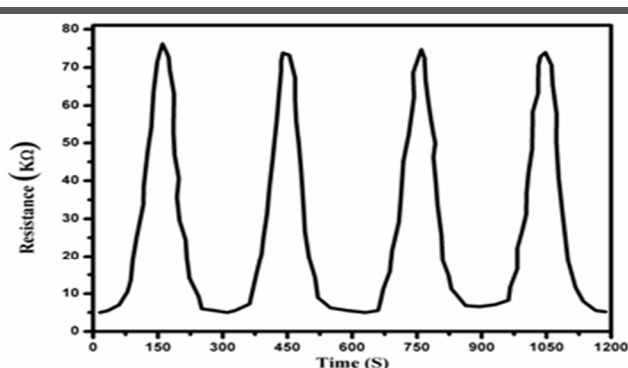


Fig. 8. Repetitive response of ZC-4 nano material to 40 ppm LPG at optimum operating temperature of 250 °C.

LPG sensing response of the ZC-4 nano material with concentrations varying from 10 to 80 ppm is shown in Fig. 9. It is observed that the gas response increased with an increase in the LPG concentration up to 40 ppm. Furthermore, the base line remains almost stable and no significant variation in the gas response is observed. The ZC-4 nano material is able to detect as low as 10 ppm for LPG with good response at the optimum

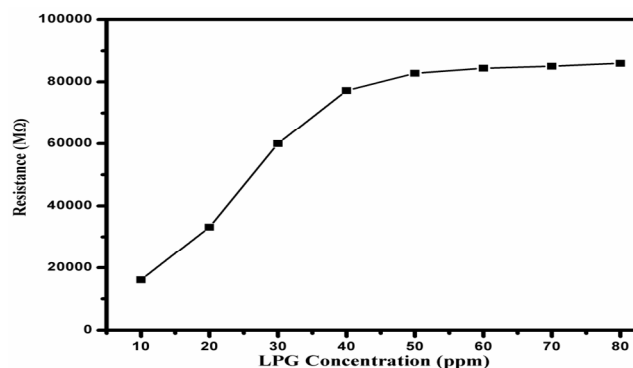


Fig. 9. Response of ZC-4 nano material upon sequential exposure to LPG with concentrations varying from 20 to 80 ppm. operating temperature of 250 °C.

Selectivity is an important parameter of gas sensors and it is the ability of a sensor to respond to a certain gas in presence of other gases. The gas sensing ability of ZC-4 nano material towards LPG, ethanol, CO, CO<sub>2</sub> and NH<sub>3</sub> with concentration 40 ppm each were also measured and results are shown in Fig. 10 (ESI Fig. S2). Among these gases highest sensible gas is LPG (~77.5), whereas it shows a considerably lower response (<18) to H<sub>2</sub>, ethanol, CO, CO<sub>2</sub> and NH<sub>3</sub>. This might be due to the adsorption of LPG gas more efficiently than others may lead to higher sensing response.

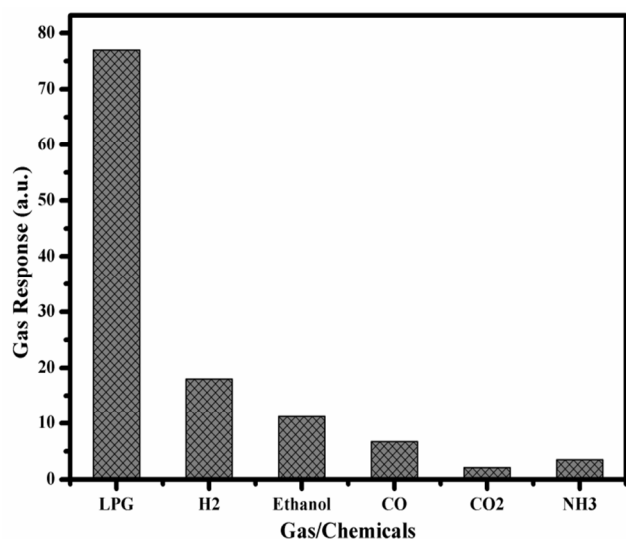
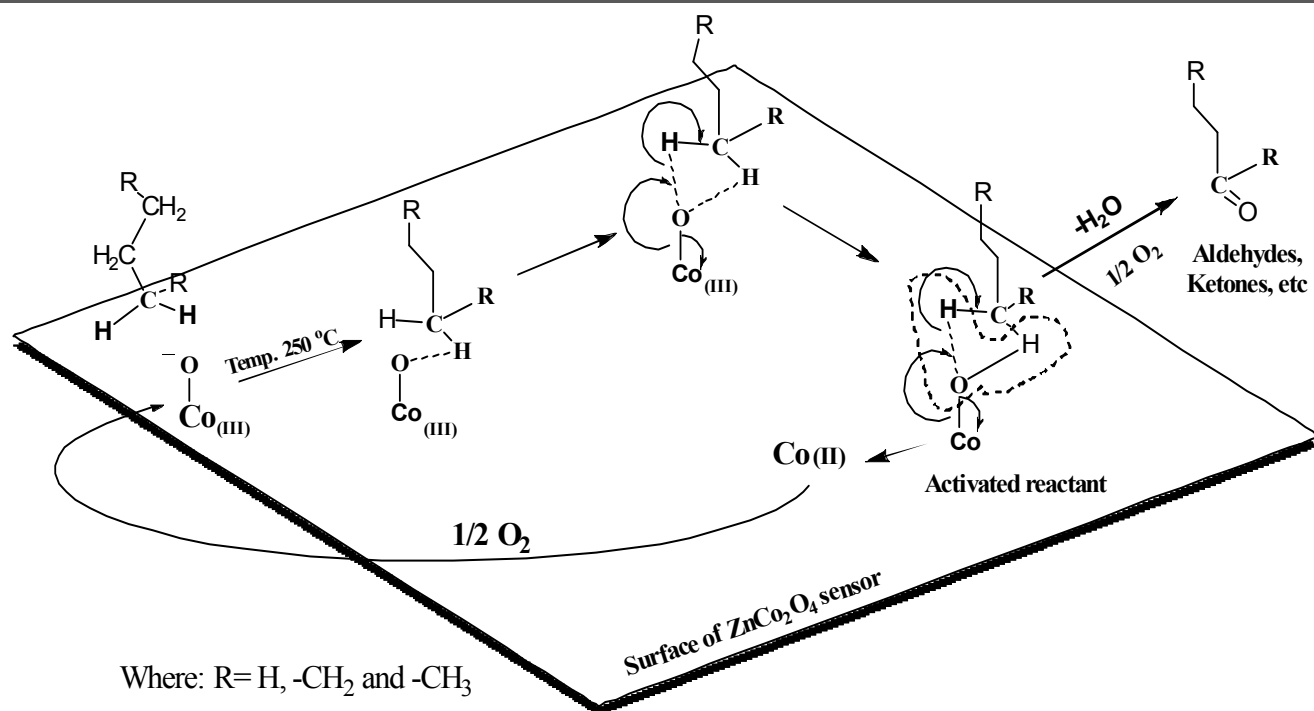


Fig. 10. Bar chart showing the gas response of ZC-4 nano material for different gases.

It is well known that in the spinel ZnCo<sub>2</sub>O<sub>4</sub>, two oxidation states viz. Zn<sup>2+</sup> and Co<sup>3+</sup> coexist and a dynamic equilibrium is set up between them and the lattice oxygen (O<sub>2</sub><sup>-</sup>) species under liquid phase oxidation conditions.<sup>29,30,43</sup> As shown in Scheme 1, sensing of gas over the surface initiate with oxidative dehydrogenation proceeds via approach/collision of gas (LPG) towards the cobalt octahedral species having lattice oxide ion.<sup>29,44-46</sup> The adsorbed LPG formed first inter-molecular bonding between surface oxide ion with hydrogen of LPG gas as shown in Scheme 1. Subsequently Co<sup>3+</sup> OH species were formed due to abstraction of hydrogen by the oxide ion.<sup>47</sup> This change in chemical states might source to increase in resistance, hence nano material show instantaneous response for chemical changes at surface. While, activated Co<sup>3+</sup> OH species were capable of forming another intermolecular hydrogen bond and abstraction of a second electron forms the major products such as oxygenated LPG (aldehyde, ketones, etc.), Co<sup>2+</sup> and water molecule. This self sweep out phenomenon resulted into decrease in resistance, thus instantaneous recovery of surface chemical states. However, the reduced Co<sup>2+</sup> species get reoxidized using molecular oxygen to form again active Co<sup>3+</sup>O<sup>-</sup> species. The lower sensing ability observed in case of ethanol, CO, CO<sub>2</sub> and NH<sub>3</sub> gas/chemicals (Fig. 10) might be due to lesser interaction of the gas/chemicals to form a intermolecular bonding with hydrogen and cobalt oxide ion either at the initial step (adsorption) or after the activation of reactant as shown in Scheme 1. Thus, results revel that interactions of gas with active sites were less in case of ethanol, CO, CO<sub>2</sub> and NH<sub>3</sub> gas/chemicals resulting in lower sensing activity.



Scheme 1. Plausible sensing pathway for ZnCo<sub>2</sub>O<sub>4</sub> nano material.

Cite this: DOI: 10.1039/c0xx00000x

www.rsc.org/xxxxxx

## PAPER

## Conclusions

In summary, a novel method to enhance the sensitivity of nanorods of ZC-4 sensor was proposed and demonstrated in this paper. The sensitivity of the sensor can be remarkably increased by increase in cobalt composition (ZnCo composite) from 1:1 to 1:2.5, which is beneficial to uniform distribution of  $\text{Co}^{3+}$  and  $\text{Zn}^{2+}$  active sites as a result of this increase in reducibility ultimately to enhance gas sensing by two times. ZC-4 nanorods have good LPG sensing properties such as fast response (~80–90 s), fast recovery time (~65–75 s), excellent repeatability (fourth cycle), good selectivity (for LPG), higher gas response (~77.5) able to detect lowest 10 ppm LPG concentration and wide operating temperature (30–250 °C). These results along with a zinc cobalt composition (1:2.5) demonstrate that surface active  $\text{Zn}^{2+}$ ,  $\text{Co}^{2+}$  and  $\text{Co}^{3+}$  species influence sensing ability are promising for large scale fabrication of simple, cost-effective and high performance LPG gas sensors operating not only at low but also at high LPG concentration and temperature.

## References

- 1 S. Vijayanand, P. A. Joy, H. S. Potdar, D. Patil and P. Patil, *Sensors Actuators B*, 2011, **152**, 121–129.
- 2 N. Wu, M. Zhao, J. G. Zheng, C. Jiang, B. Myers, S. Li, M. Chyu and S.X. Mao, *Nanotechnology*, 2005, **16**, 2878–2881.
- 3 A. Srivastava and R. K. Jain, *Mater. Chem. Phys.*, 2007, **105**, 385–390.
- 4 W. J. Moon, J. H. Yu and G.M. Choi, *Sensors Actuators B Chem.*, 2002, **87**, 464–470.
- 5 T. Zhang, L. Liu, Q. Qi, S. Li and G. Lu, *Sensors Actuators B Chem.*, 2009, **139**, 287–291.
- 6 K. I. Choi, H. R. Kim and J.H. Lee, *Sensors Actuators B Chem.*, 2009, **138**, 497–503.
- 7 B. Bahrami, A. Khodadadi, M. Kazemeini and Y. Mortazavi, *Sensors Actuators B Chem.*, 2008, **133**, 352–356.
- 8 L. Zhang, J. Hu, P. Song, H. Qin, K. An, X. Wang and M. Jiang, *Sensors Actuators B Chem.*, 2006, **119**, 315–318.
- 9 C. C. Wang, S. A. Akbar and M. J. Madou, *J. Electroceram.*, 1998, **2**, 273–282.
- 10 N. Barsan and U. Weimar, *J. Electroceram.*, 2001, **7**, 143–167.
- 11 Y. Suna, L. Zhanga, J. Zhanga, P. Chena, S. Xina, Z. Lib and J. Liu, *Ceram. Int.*, 2014, **40**, 1599–1603.
- 12 J. X. Wang, X. W. Sun, H. Huang, Y. C. Lee, O. K. Tan, M. B. Yu, G. Q. Lo and D. L. Kwong, *Appl. Phys. A*, 2007, **88**, 611–615.
- 13 Y. Jia, L. He, Z. Guo, X. Chen, F. Meng, T. Luo, M. Li and J. Liu, *J. Phys. Chem. C*, 2009, **113**, 9581–9587.
- 14 X. Liu, C. Zhou, C. Li, D. Zhang, B. Lei and S. Han, *J. Phys. Chem. B*, 2003, **107**, 12451–12455.
- 15 X. Gou, G. Wang, J. Yang, J. Park and D. Wexler, *J. Mater. Chem.*, 2008, **18**, 965–969.
- 16 Q. Wan, T. H. Wang, C. C. Li, Z. F. Du, L. M. Li and H.C. Yu, *Appl. Phys. Lett.*, 2007, **91**, 032101.
- 17 R. B. Waghulade, R. Pasricha and P.P. Patil, *Talanta*, 2007, **72**, 594–599.
- 18 N. B. Sonawane, R. R. Ahire, K. V. Gurav, J. H. Kim and B. R. Sankapal, *J. Alloys Compd.*, 2014, **592**, 1–5.
- 19 M. S. Dhingra, N. K. Singh, S. Shrivastava, P. S. Kumar and s. Annapoorni, *Sensors Actuators, A Phys.*, 2013, **190**, 168–175.
- 20 S. Nath, S. S. Nath and R. K. Kumar, *J. Anal. Sci. Technol.*, 2012, **3(1)**, 85–94.
- 21 R. B. Ravikiran B., G. Arindam, G. Anil, S. Fouran and Sharma, *Sensors Actuators, B Chem.*, 2011, **160(1)**, 1050–1055.
- 22 R. J. Deokate, D. S. Dhawale and C. D. Lokhande, *Sensors Actuators, B Chem.*, 2011, **156(2)**, 954–960.
- 23 R. Aad, V. Simic, L. Le Cunff, L. Rocha, V. Sallet, C. Sartet, A. Lussou, C. Couteau and G. Lerondel, *Nanoscale*, 2013, **5**, 9176–9180.
- 24 D. C. Pugh, E. J. Newton, A. J. T. Naik, S. M. V Hailes and I. P. Parkin, *J. Mater. Chem. A*, 2014, **2**, 4758–4764.
- 25 P. Wang, Y. Fu, B. Yu, Y. Zhao, L. Xing and X. Xue, *J. Mater. Chem. A*, 2015, **3**, 3529–3535.
- 26 Y. Liu, J. Dong, P. J. Hesketh and M. Liu, *J. Mater. Chem.*, 2005, **15**, 2316–2320.
- 27 M. V Reddy, G. V Subba Rao and B. V. R. Chowdari, *Chem. Rev.*, 2013, **113**, 5364–5457.
- 28 M. V Reddy, Z. Beichen, K. P. Loh and B. V. R. Chowdari, *CrystEngComm*, 2013, **15**, 3568–3574.
- 29 A. Bielski and J. Haber, *Catal. Rev. Sci. Eng.*, 1979, **19**, 1–41.
- 30 V. R. Mate, A. Jha, U. D. Joshi, K. R. Patil, M. Shirai and C. V. Rode, *Appl. Catal. A Gen.*, 2014, **487**, 130–138.
- 31 S. R. Kadam, V. R. Mate, R. P. Panmand, L. K. Nikam, M. V. Kulkarni, R. S. Sonawane and B. B. Kale, *RSC Adv.*, 2014, **4**, 60626–60635.
- 32 V. R. Mate, M. Shirai and C. V. Rode, *Catal. Commun.*, 2013, **33**, 66–69.
- 33 D. Patil, P. Patil, S. Vijayanand, P. A. Joy and H. S. Potdar, *Talanta*, 2010, **81**, 37–43.
- 34 G. Pantaleo, G. Deganello, L. F. Liotta and G.D. Carlo, *Catal. Commun.*, 2006, **5**, 329–336.
- 35 C. G. Gao, D. S. Liu, Y. Z. Wang and Y. X. Zhao, *Catal. Lett.*, 2007, **116**, 136–142.
- 36 C. V. Chenck, J. G. Dillard and J. W. Murray, *J. Colloid Interf. Sci.*, 1983, **95**, 398–409.
- 37 M. Oku and Y. Sato, *Appl. Surf. Sci.*, 1992, **55**, 37–41.
- 38 J. Yang, H. Liu, W. N. Martens and R. L. Frost, *J. Phys. Chem. C*, 2009, **114**, 111.
- 39 K. Omata, T. Takada and S. Kasahara, *J. Appl. Catal. A Gen.*, 1996, **146**, 255–267.
- 40 T. J. Chuang, C. R. Brundle and D.W. Rice, *Surf. Sci.*, 1976, **59**, 413–429.
- 41 I. Grohmann, B. Peplinski and W. Unger, *Surf. Interface Anal.*, 1992, **19**, 591–594.
- 42 D. G. Klissurski and E. L. Uzunova, *J. Mater. Sci. Lett.*, 1990, **9**, 576–579.
- 43 J. J. Rehr, S. D. Conradson, A. L. Ankudinov and B. Ravel, *Phys. Rev. B*, 1998, **58**, 7565–7576.
- 44 P. A. Rock, *Inorg. Chem.*, 1968, **7**, 837–840.
- 45 R. A. Sheldon and R.A. van Santen, *Catalytic Oxidation: Principles and Applications*, World Scientific, Singapore, 1995.
- 46 G. Centi, F. Cavani, F. Trifiro and M. V. Twigg, *Fundamental and Applied Catalysis Selective Oxidation by Heterogeneous Catalysis*, KluwerAcademic/Plenum Publishers, New York, 2001.
- 47 B. Gillot, M. Laarj, P. Tailhades and A. Rousset, *Mater. Chem. Phys.*, 1988, **19**, 485–495.